Combustion, Explosion, and Shock Waves, Vol. 43, No. 1, pp. 56–61, 2007

Effect of a Heat-Conducting Element on the Gasless Combustion of Cylindrical Samples under Nonadiabatic Conditions

V. G. Prokof'ev,[1] A. V. Pisklov,[1] and V. K. Smolyakov[1]

UDC 536.46

Translated from *Fizika Goreniya i Vzryva*, Vol. 43, No. 1, pp. 66–71, January–February, 2007.
Original article submitted November 2, 2005; revision submitted May 24, 2006.

The effect of a heat-conducting element on the ignition and combustion of a cylindrical layer of a gasless mixture with a nonadiabatic lateral surface is studied. It is shown that the introduction of an element with high heat conductivity allows one to extend the region of ignition of the gasless composition by a heated surface and to increase burning rate under conditions of external heat release.

Key words: functional gradient materials, gasless combustion, heat-conducting element, unsteady regimes, heat losses.

INTRODUCTION

An effective method of increasing the burning rate of a condensed system involves the use of heat-conducting elements (HCEs) made of metals with high heat-conducting properties. By introducing a HCE in the form of a metal wire into a mixed composition or a pyrotechnic composition, it is possible to increase the burning rate by a factor of 2 to 3 [1]. The increase in the burning rate is due to an increase in the burning surface area of the propellant, for example, as a result of mechanical destruction of the sample [2], or it is due to an increase in the effective heat conductivity of the system [3]. The heat for heating the HCE comes from the gas-phase combustion products of the condensed system. Another application of HCEs is the combustion synthesis of functionally gradient materials (FGMs) using primarily gasless compositions. Because of a nonuniform distribution of the components of the reactive mixture, a material with specified physicochemical properties is produced, whose constructional internal element is a HCE. In practice, FGMs are produced using compositions with a continuous nonuniform distribution of components without macroscopic boundaries between the layers. Unlike in the combustion of pyrotechnic compositions, in the combustion of layered SHS compositions, the heat for heating the HCE or layers of low calorific value comes from the condensed reaction products.

Numerical studies [4–6] of solid-flame combustion of a homogeneous cylindrical sample in a three-dimensional formulation show that there are a variety of unsteady combustion regimes under both adiabatic and nonadiabatic conditions. The structure of the combustion wave of a cylindrical sample of a metal-thermite composition enclosed in a cylindrical shell of a material with thermal insulation properties was studied in a two-dimensional formulation in [7, 8]. The one-dimensional propagation of the combustion front in a nonuniform medium containing an inert low-melting component was studied theoretically in [9] as applied to the problem of the combustion synthesis of FGMs.

In the present paper, we consider the gasless combustion of a compound sample consisting of a cylindrical layer of a reactive material with a nonadiabatic outer boundary and an inner core made of an inert material with high heat-conducting properties. In view of the high heat conductivity of the core, the influence of the circumferential heat-transfer component on combustion-wave propagation is ignored in comparison with the longitudinal and radial components.

[1]Tomsk State University, Tomsk 634050; pvg@ftf.tsu.ru.

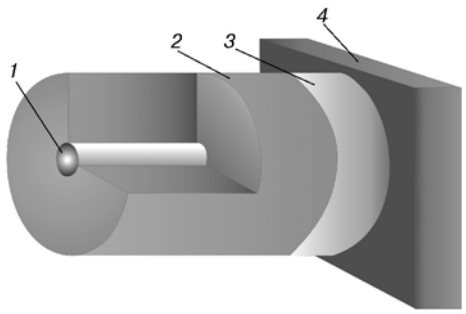

Fig. 1. Experimental layout: 1) HCE; 2) starting reactive material; 3) condensed reaction products; 4) heated surface.

FORMULATION OF THE PROBLEM

The combustion of a cylindrical layer of a gasless composition with an internal heat-conducting element in the form of a coaxial cylinder is considered. The inner radius of the reaction layer and the radius of the core coincide. Ignition is carried out by a heated surface at the end face of the cylinder in two versions: 1) contact of the heated surface with the reactive material and thermal insulation at the end of the core; 2) simultaneous heating of the reactive material and the core. Initiation of combustion by means of contact of the heated surface only with the core occurs with a large induction period; therefore this ignition method is not considered. The opposite end face is assumed to be heat insulated. Conditions of heat transfer to the ambient medium are imposed on the lateral surface of the cylinder. The synthesis of FGMs is characterized by a continuous variation of the mixture components, resulting in a continuous or a piecewise-continuous distribution of the thermophysical constants in the sample. The experimental layout is given in Fig. 1.

The mathematical model in a two-dimensional axisymmetric formulation includes the following equations in dimensionless form:
the heat-conduction equation

$$c(\xi)\,\frac{\partial\theta_i}{\partial\tau} = \frac{1}{\xi}\,\frac{\partial}{\partial\xi}\Big(\lambda(\xi)\,\xi\frac{\partial\theta_i}{\partial\xi}\Big) + \\ + \lambda(\xi)\,\frac{\partial^2\theta_i}{\partial z^2} + \frac{1}{\gamma}\,\frac{\partial\eta}{\partial\tau}\,e(\xi-\xi_0); \qquad (1)$$

the chemical kinetics equation in the region $\xi_0 < \xi \leqslant R$

$$\frac{\partial\eta}{\partial\tau} = \gamma(1-\eta)\exp\frac{\theta_2}{1+\beta\theta_2}; \qquad (2)$$

the distribution of thermophysical constants

$$\lambda(\xi) = \Lambda e(\xi_0-\xi) + e(\xi-\xi_0),$$
$$c(\xi) = \Omega e(\xi_0-\xi) + e(\xi-\xi_0), \qquad (3)$$

$$e(\xi-\xi_0) = \begin{cases} 1, & \xi > \xi_0, \\ 0, & \xi < \xi_0. \end{cases}$$

The boundary conditions are as follows:

$$\text{for } \tau \leqslant \tau_{\text{ign}}, \quad \begin{cases} \theta_2(0,\xi,\tau) = 0, \\ \dfrac{\partial\theta_1(0,\xi,\tau)}{\partial z} = 0, \end{cases} \qquad (4)$$
$$\text{or} \quad \theta_i(0,\xi,\tau) = 0;$$

$$\text{for } \tau > \tau_{\text{ign}}, \quad \frac{\partial\theta_i(0,\xi,\tau)}{\partial z} = 0;$$

$$\text{for } \xi = \xi_0, \quad \theta_1 = \theta_2, \quad \Lambda\,\frac{\partial\theta_1}{\partial\xi} = \frac{\partial\theta_2}{\partial\xi}, \qquad (5)$$

$$\frac{\partial\theta_i(L,\xi,\tau)}{\partial z} = 0, \qquad (6)$$
$$\frac{\partial\theta_2(z,R,\tau)}{\partial\xi} + \alpha_t[\theta_2(z,R,\tau)-\theta_0] = 0,$$

$$\theta_i(z,\xi,0) = \theta_0, \quad \eta(z,\xi,0) = 0. \qquad (7)$$

Here the subscripts $i = 1$ and 2 refer to the inert material of the HCE and reactive material, respectively. The following variables and parameters traditional for combustion problems are used:

$$\gamma = \frac{c_2R_{\text{g}}T_*^2}{QE}, \quad \beta = \frac{R_{\text{g}}T_*}{E},$$
$$\theta = \frac{(T-T_*)E}{R_{\text{g}}T_*^2}, \quad \theta_0 = \frac{(T_0-T_*)E}{R_{\text{g}}T_*^2},$$
$$\Lambda = \frac{\lambda_1}{\lambda_2}, \qquad \Omega = \frac{c_1\rho_1}{c_2\rho_2}, \quad \xi = \frac{r}{r_*}, \quad \xi_0 = \frac{r_0}{r_*},$$
$$r_* = \sqrt{\frac{\lambda_2 t_*}{c_2\rho_2}}, \quad t_* = \frac{c_2R_{\text{g}}T_*^2}{QEk_0}\exp\frac{E}{R_{\text{g}}T_*},$$
$$\alpha_t = \frac{\alpha r_*}{\lambda_2}, \quad \tau = \frac{t}{t_*}, \quad \tau_{\text{ign}} = \frac{t_{\text{ign}}}{t_*},$$
$$R = \frac{R_0}{r_*}, \quad L = \frac{l}{r_*}, \quad z = \frac{x}{r_*}.$$

Here ρ is the density, c is the heat capacity, λ is the thermal conductivity, R_0 and r_0 are the dimensional radii of the sample and the heat-conducting element, respectively, l is the dimensional length of the sample, σ is the ratio of the radius of the heat-conducting element to the radius of the sample, R_{g} is the universal gas constant, Q, E, and k_0 are the heat effect of the reaction, the activation energy, and the preexponent, α and α_t are the dimensional and dimensionless heat-transfer coefficients t_{ign} and τ_{ign} are the dimensional and dimensionless times of action of the heater, θ and θ_0 are the local and initial dimensionless temperatures, η is the degree of conversion, t_* and x_* are the time

and coordinate scales, τ, ξ, and z are the dimensionless time and the radial and longitudinal coordinates, β and γ are dimensionless parameters, Ω and Λ are the ratios of the thermophysical constants, and $e(\xi - \xi_0)$ is a unit function. The scale temperature is equal to

$$T_* = T_0 + \frac{Q}{c_2} - \frac{1}{2}\frac{R_g T_*^2}{E}.$$

For the cylindrical sample, the following dimensionless parameters are used: L is the length of the cylinder generatrix, R is the outer radius of the cylinder, and ξ_0 is the radius of the HCE and the inner radius of the cylindrical layer of the reactive material.

The system of equations was solved numerically using the coordinate splitting method with an implicit scheme. The boundary between the inert and reactive media was located between the nodes of the computational grid. The thermal flows were approximated using central differences. The calculations were performed on a uniform grid with a time step of 0.05 and a space step of 0.2. The approximation convergence was checked by refining the computational grid. The error in calculating the burning time of the layer did not exceed 1%. The thermophysical parameters $\Lambda = 38$ and $\Omega = 1.8$ corresponded to the following materials: Cu for the heat-conducting element, and Nb–2B for the reactive material. It should be noted that the adiabatic combustion temperature of the Nb–2B system reaches 2300 K [10]. At this temperature, the inert material of the core is in a molten state. The formation and spread of the melt over the starting mixture was ignored in the present homogeneous model. The time of contact of the sample with the heated surface was set equal to $\tau_{\text{ign}} = 200$.

CALCULATION RESULTS

Steady-State Combustion Regime

The main purpose of the calculations was to determine the time of complete combustion of the reaction layer τ_b. The calculated values of τ_b were compared with the time τ_b^0 of complete combustion of a homogeneous cylindrical sample ($\xi_0 = 0$). The position of the combustion front was determined by computation points with a degree of conversion equal to 0.9. The combustion front was curved with the largest curvature observed near the core. Two versions of the development of the combustion wave are possible, depending on the external heat-transfer level and the ratio of the dimensions of the core and the reaction layer: complete combustion of the reaction layer and combustion quenching at a distance from the heated wall. In the range of parameter

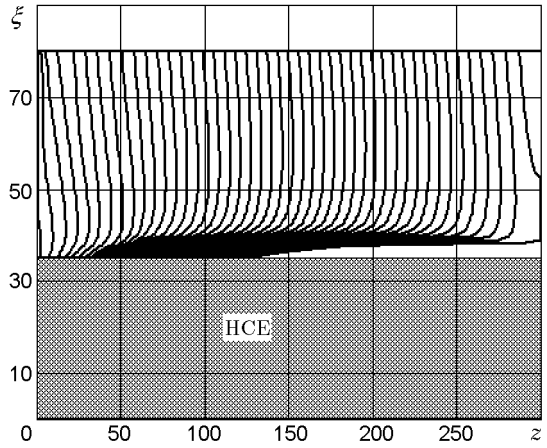

Fig. 2. Steady-state combustion regime. Ignition upon complete contact of the heated surface and the sample. Positions of combustion front at various times ($\Delta\tau = 30$): $\theta_0 = -6$, $\beta = 0.1$, $\alpha_t = 0.02$, $R = 80$, $\xi_0 = 35$, and $L = 300$.

values corresponding to a one-dimensional steady-state combustion wave [11], steady-state (except during the ignition and afterburning of the sample) combustion occurs (Fig. 2). In the ignition stage until the switching-off of the heated walls (complete contact of the end face with the wall), the burning surface has a weakly expressed conical shape, which is a consequence of the higher heat conductivity of the core. After the external heating is switched off, the burning surface is leveled. The propagation of the combustion front along the core surface is decelerated. Beginning at the ignition time, a steady-state combustion regime is established, in which the burning rate and temperature at all points of the front vary only slightly in time. This combustion regime can exist only until the attainment of certain values of the ratio of the dimensions of the reaction layer and the core $\sigma = \xi_0/R$ and the heat-transfer coefficient α_t. An increase in the radius ξ_0 above a critical value with the values of R and α_t remaining unchanged leads to combustion quenching. The propagation of the combustion wave in the longitudinal direction is accompanied by an increase in the volume of unreacted material near the core. Before combustion quenching, the frontal surface has a conical shape with the top on the HCE and an increasing radius of the base (Fig. 3). The minimum burning rate before quenching differs from the burning rate of the homogeneous sample under adiabatic conditions by a factor of approximately 1.4, which agrees with the analytical conclusions of [12] for gas flames.

The dependence of the burning time of the reaction layer on the radius of the core is nonmonotonic (curve 1 in Fig. 4). At a ratio of the radii $\sigma \approx 0.3$, the burn-

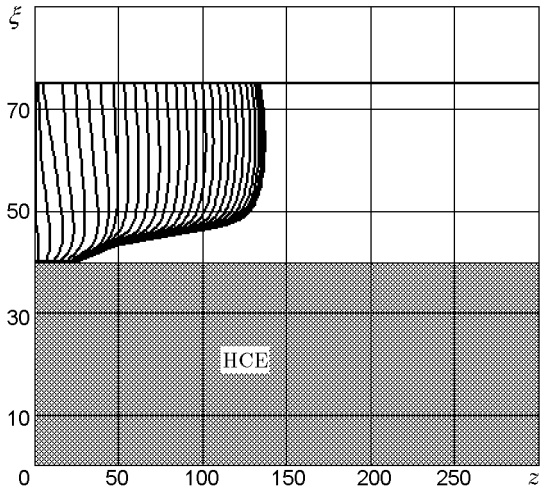

Fig. 3. Combustion quenching. Ignition upon complete contact of the heated surface with the sample. Positions of the combustion front at various times ($\Delta\tau = 30$): $\theta_0 = -6$, $\beta = 0.1$, $\alpha_t = 0.02$, $R = 75$, $\xi_0 = 40$, and $L = 300$.

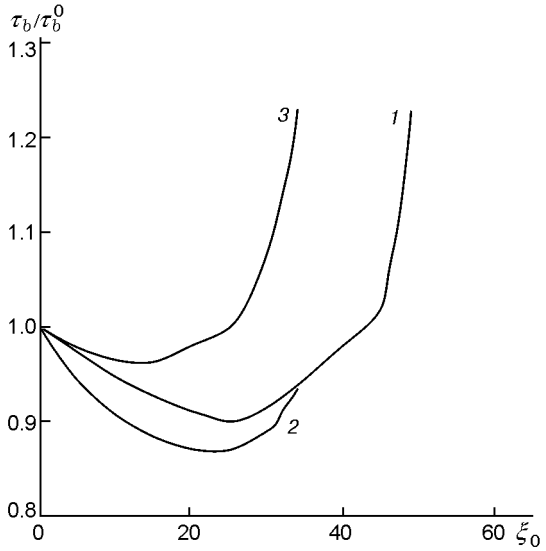

Fig. 4. Burning time of the sample versus the radius of the HCE: $R = 80$, $\beta = 0.1$, $\alpha_t = 0.02$, $L = 300$; curve 1 refers to $\theta_0 = -6$, curve 2 refers to $\theta_0 = -7$ (ignition upon complete contact of the heated surface with the sample), and curve 3 refers to $\theta_0 = -6$ (contact of the heated surface only with the reactive material).

ing time of the layer is 10% smaller than the burning time of the homogeneous cylindrical sample. The effectiveness of the core increases with a relative increase in the heat-conducting properties of the core material. The ignition version with the thermal insulation of the HCE and the heated surface is less effective (curve 3 in Fig. 4) than ignition upon complete contact of the end face of the sample with the wall. During heating, the heat transfer from the wall to the HCE is higher (due to the higher heat conductivity) than the heat transfer to the same volume of the reaction layer, and this facilitates combustion-wave propagation in the initial stage. However, as the combustion wave propagates over the sample, the core changes from a heat source to a heat sink. The value $\sigma \approx 0.6$ is critical, and for larger values, complete combustion of the reaction layer for the given set of parameters becomes impossible. A decrease in the heat-transfer coefficient α_t extends the combustion limits in σ.

Unsteady Combustion Regime

As the initial temperature θ_0 decreases, the combustion regime becomes unsteady. The typical variation in the temperature field in the axial section for the pulsating combustion regime is presented in Fig. 5. In the cross section through the reaction zone, the temperature of the core is three characteristic intervals below the maximum temperature in the center. At the same time, in the heating zone, the temperature of the inert material is on the average 1.5 interval higher than the temperature of the reactive material, which is responsible for the large curvature of the burning surface near the core. The combustion source moves from the outer surface of the sample, expanding toward the core, but it does not reach the core surface. An unburned material layer (Fig. 6) is formed near the core. The stage of predominantly radial motion of the combustion source is followed by a depression stage with the formation of a heated layer. The next run of the combustion source in the radial direction occurs after burnout of an outer surface region of the reactive material. The unburned layer formed on the core surface also reacts in a pulsating regime and completely burns up in the final phase of the sample combustion. The oscillation amplitude of the longitudinal component of the burning rate near the core is twice that on the lateral surface of the sample. The oscillation period remains unchanged over the width of the reaction layer. A similar variation in the oscillation amplitude with distance from the inert shell with doubled period is reported in [7].

It is characteristic that for the homogeneous sample containing no inert HCE, initiation of combustion with the displacement of the one-dimensional front to the instability region and with the preservation of heat loss level is not possible even when the time of contact with the heated wall is increased many times. Furthermore, the use of a core of a rather small radius ξ_0 does not make it possible to implement steady-state propagation of the combustion wave for a fixed time of con-

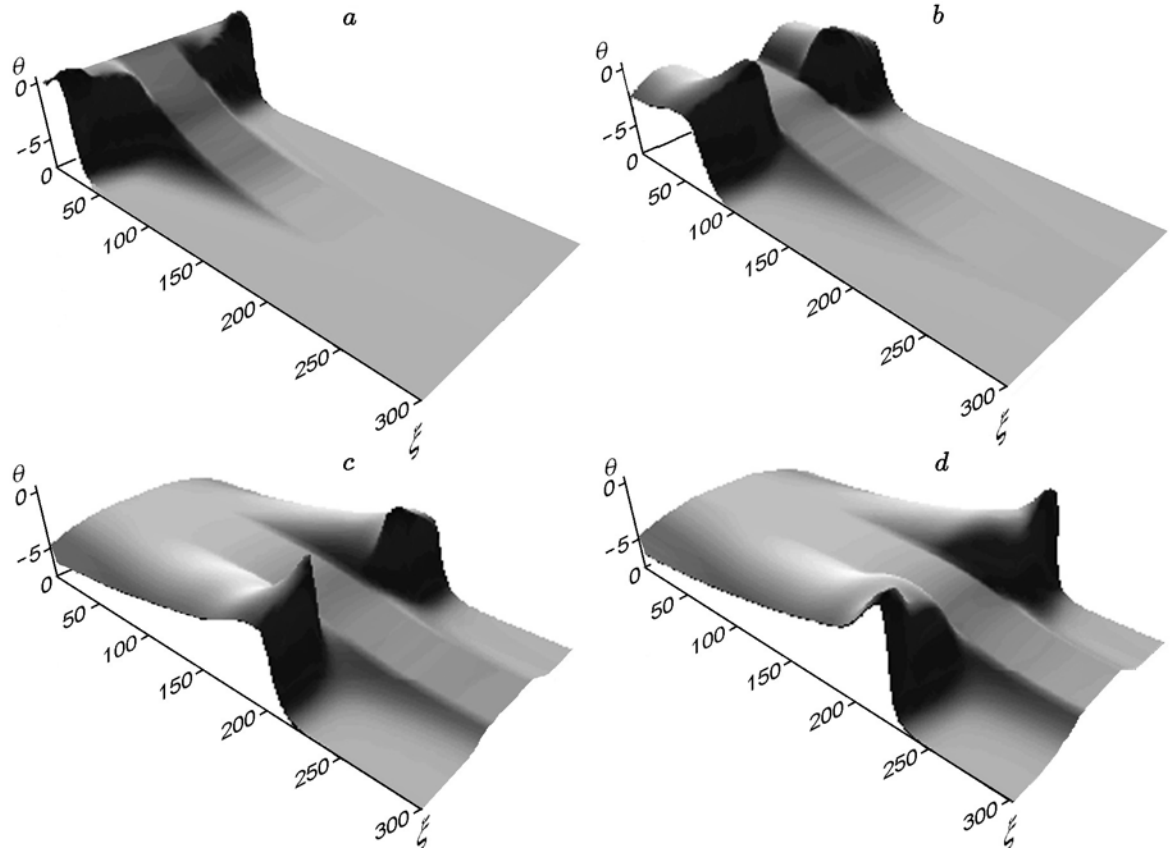

Fig. 5. Temperature distribution in the axial section of the sample. Ignition upon complete contact of the surface with the sample ($\theta_0 = -7.5$, $\beta = 0.1$, $\alpha_t = 0.02$, $R = 80$, $\xi_0 = 25$, and $L = 300$) for $\tau = 200$ (a), 540 (b), 1481.3 (c), and 1613.3 (d).

tact with the wall, which, in fact, is a problem on the critical ignition conditions. Combustion of the entire reactive material at $\tau_{\text{ign}} = 200$ and $\theta_0 = -7.5$ can be initiated with cores of radius $\xi_0 \geqslant 22$. Increasing ξ_0 leads to an increase in the initial burning rate due to the heat accumulated by the core; in this case, however, the thickness of the unburned layer on the surface of the inert element increases. The further propagation of the combustion wave is accompanied by a decrease in the longitudinal component of the burning rate due to the external and internal heat transfer before combustion quenching. Combustion quenching occurs, as in the one-dimensional case, in the depression stage. Complete transformation of the reaction layer can be achieved by using a core of radius $22 \leqslant \xi_0 \leqslant 27$. The lower boundary of the indicated range of ξ_0 depends on τ_{ign} and L. The region of steady ignition is extended by increasing the time of contact with the wall. In contrast, increasing L for a fixed time of contact with the wall leads to a decrease in the average temperature of the inert rod, and the thickness of the unburned material layer on the core surface increases. The effectiveness of using the HCE [3] in gasless combustion increases as the initial temperature θ_0 is decreased (see Fig. 4). Combustion of the cylindrical layer of the reactive material with the complete preservation of the heat-transfer coefficient α_t becomes impossible with a further decrease in θ_0.

CONCLUSIONS

1. The introduction of the heat-conducting element to the gasless composition in the examined range of parameters does not lead to a considerable increase in the burning rate, as is observed for model pyrotechnic compositions.

2. In the presence of heat losses, the heat-conducting element facilitates the activation of synthesis in the cylindrical layer of the reactive material.

3. An increase in the radius of the heat-conducting element can lead to the formation of an unburned material layer on its surface.

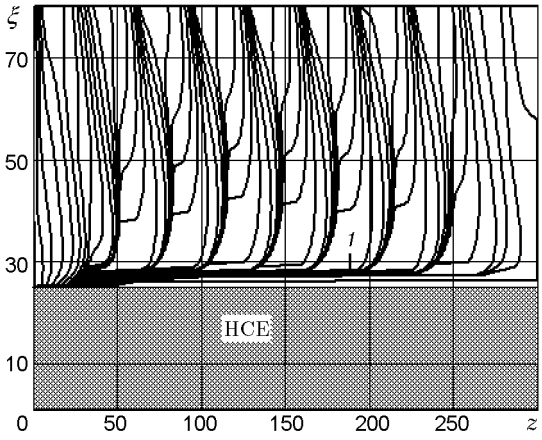

Fig. 6. Pulsating combustion regime. Ignition upon complete contact of the heated surface with the sample. Positions of the combustion front at various times ($\Delta\tau = 30$): $\theta_0 = -7.5$, $\beta = 0.1$, $\alpha_t = 0.02$, $R = 80$, $\xi_0 = 25$, and $L = 300$; segments of curves showing the unburned layer are marked by 1.

4. There is an optimum value of the diameter of the heat-conducting element for which the average burning rate of the gasless composition sample is maximal.

This work was supported by the Russian Foundation for Basic Research (Grant No. 05–08-01396a).

REFERENCES

1. N. N. Bakhman and I. N. Lobanov, "Effect of heat-conducting elements on burning rate," *Combust., Expl., Shock Waves*, **11**, No. 3, 424–428 (1975).
2. V. A. Arkhipov, A. K. Abushaev, and V. F. Trofimov, "Combustion of condensed substances reinforced by elements with the shape memory effect," *Combust., Expl., Shock Waves*, **32**, No 3, 291–295 (1996).
3. N. N. Bakhman and I. N. Lobanov, "Influence of the diameter of the heat-conducting elements on their efficiency during the of condensed systems," *Combust., Expl., Shock Waves*, **19**, No. 1, 42–46 (1983).
4. T. P. Ivleva and A. G. Merzhanov, "Three-dimensional modeling of solid-flame chaos," *Dokl. Akad. Nauk*, **381**, No. 2, 210–213 (2001).
5. T. P. Ivleva and A. G. Merzhanov, "Mathematical simulation of three-dimensional spin regimes of gasless combustion," *Combust., Expl., Shock Waves*, **38**, No. 1, 41–48 (2002).
6. T. P. Ivleva and A. G. Merzhanov, "Three-dimensional unsteady solid flame combustion under nonadiabatic conditions," *Combust., Expl., Shock Waves*, **39**, No. 3, 300–308 (2003).
7. B. L. Kopeliovich, "Combustion of gas-free mixture in narrow cylindrical channel," *Combust., Expl., Shock Waves*, **31**, No. 5, 532–536 (1995).
8. B. L. Kopeliovich, "Origination of reaction sites in the front of gasless combustion under the action of heat losses," *Combust., Expl., Shock Waves*, **39**, No. 6, 650–655 (2003).
9. V. K. Smolyakov and V. G. Prokofiev, "The theory of self-propagating high-temperature synthesis of functionally gradient materials," *Int. J. SHS*, **12**, No. 1, 1–9 (2003).
10. A. G. Merzhanov, *Solid-Flame Combustion* [in Russian], Izd. ISMAN, Chernogolovka (2000).
11. K. G. Shkadinskii, B. I. Khaikin, and A. G. Merzhanov, "Propagation of a pulsating exothermic reaction front in the condensed phase," *Combust., Expl., Shock Waves*, **7**, No. 1, 15–22 (1971).
12. Ya. B. Zel'dovich, "Theory of the propagation limit of a quiet flame," *Zh. Éksp. Teor. Fiz.*, **11**, No. 1. 159–168 (1941).